



# **An Introduction to the Simulation of MIMO Systems with WinProp**

*Responsible Editor:*

*Oliver Stäbler*

*AWE Communications GmbH*

*Otto-Lilienthal-Str. 36*

*D-71034 Böblingen*

*Phone: +49 70 31 71 49 7 - 19*

*Fax: +49 70 31 71 49 7 - 12*

*[Oliver.Staebler@AWE-Communications.com](mailto:Oliver.Staebler@AWE-Communications.com)*

## Content

1	Motivation.....	3
2	Wave Propagation .....	4
3	Contribution and Superposition of Rays .....	7
4	Ray Data Files .....	10
4.1	ASCII Ray Files for Indoor Scenarios.....	12
4.2	ASCII Ray Files for Urban Scenarios .....	13
5	Further MIMO specific Channel Parameters.....	14
5.1	MIMO Channel Matrix.....	14
5.2	MIMO Channel Capacity.....	16
6	One Possibility to Determine Additional Channel Parameters related to MIMO Systems .....	18
6.1	Selections concerning the simulation area .....	18
6.2	Adjustment of the Tx MIMO Antenna Array .....	20
6.3	Adjustment of the Rx MIMO Antenna Array .....	22
6.4	Output Options .....	24
6.5	Further options .....	26
7	Other Applications .....	27
8	Further Information .....	28
9	References.....	28

## History

<i>Issue</i>	<i>Date</i>	<i>Changes</i>
V1	11/23/2007	First version of document

# 1 Motivation

In the last few years multiple-input multiple-output (MIMO) systems, which deploy spatially separated multiple antenna elements at both ends of the transmission link, have emerged as one of the most promising approaches for high data rate and more reliable wireless systems. It was shown that the MIMO channel capacity grows linearly with antenna pairs as long as the environment has sufficiently rich scatterers. According to this the capacity gains ultimately depend on the propagation channel in which the system is operating. For attaining or at least approaching those capacities, sophisticated signal processing algorithms and coding strategies have been developed and corresponding research is on going. In order to assess the benefits and possible problems of these algorithms, realistic models of the wireless propagation channel are required. Hence, the establishment of good spatial channel models is essential both for the development of new algorithms for signal processing, modulation, coding, and for the unified testing of different system proposals in standardization.

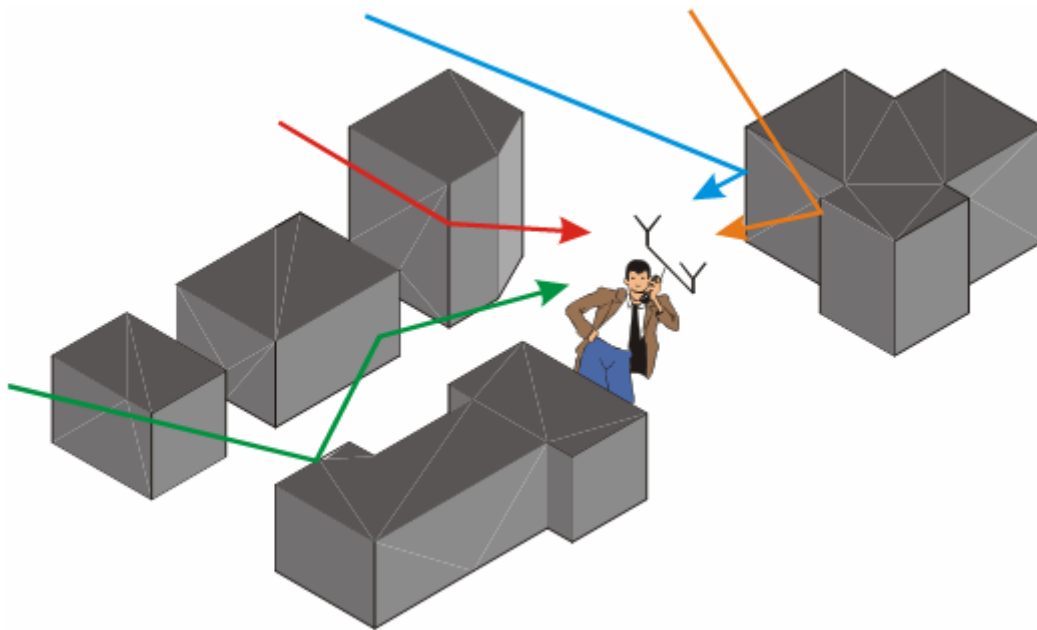


Figure 1: MIMO Scheme

AWE Communication's radio planning tool WinProp has been upgraded towards the consideration of MIMO systems.

## 2 Wave Propagation

MIMO channel capacity grows linearly with the number of antenna pairs as long as the environment has sufficiently rich scatterers. Thus highly accurate wave propagation models are required to evaluate the MIMO channel parameters in complex modeled propagation scenarios. The radio network planning tool of AWE Communications includes ray-optical wave propagation models which process 3D vector data of buildings in order to determine the mobile radio channel within various environments (rural, urban, and indoor). For the consideration of MIMO antenna arrays the tool allows the prediction of the radio channel in time, frequency, and spatial domains between each pair of the BS and MS antenna elements. Furthermore the ray tracing model was extended to consider vertical and horizontal polarization which influences the transmission, reflection and diffraction coefficients (e.g. according to Fresnel coefficients and geometrical/uniform theory of diffraction (GTD/UTD)).

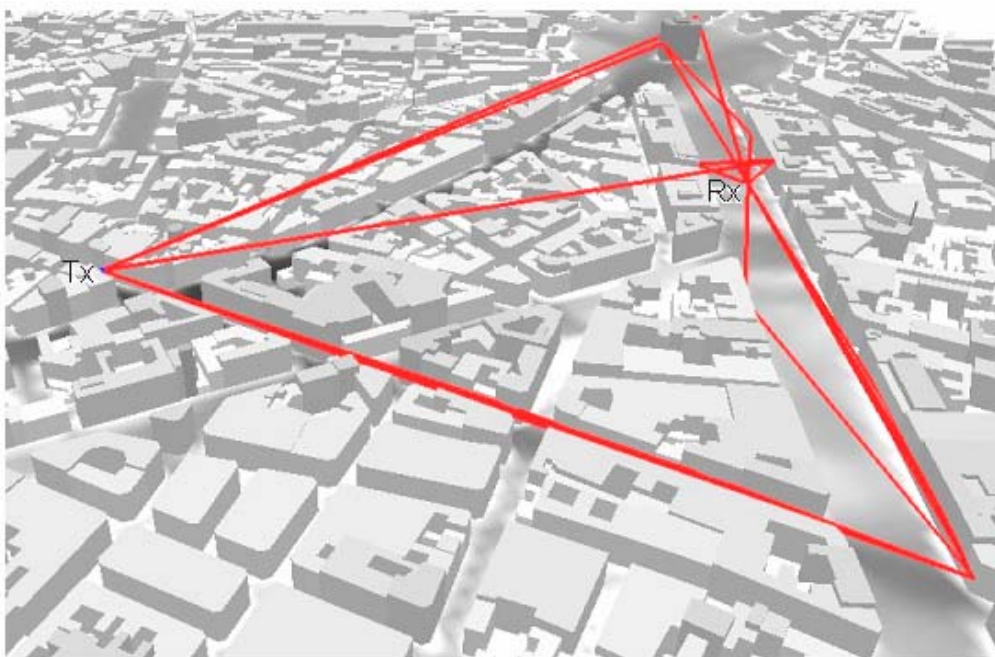
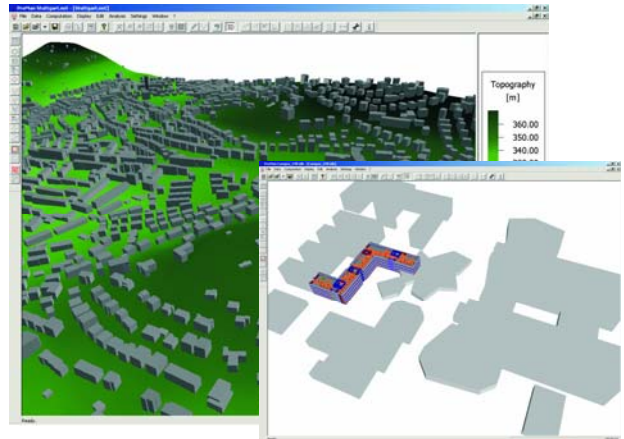


Figure 2: Ray tracing in urban scenario

Ray-optical propagation models provide accurate site specific and easily reproducible information and cope with effects such as shadowing behind walls, wave guiding in street canyons (see Figure 3), offer excellent accuracy and are able to provide additional parameters such as small-scale fading, and the angles of departure (AoD) as well as angles of arrival (AoA) which are relevant for the analysis of the MIMO channel.

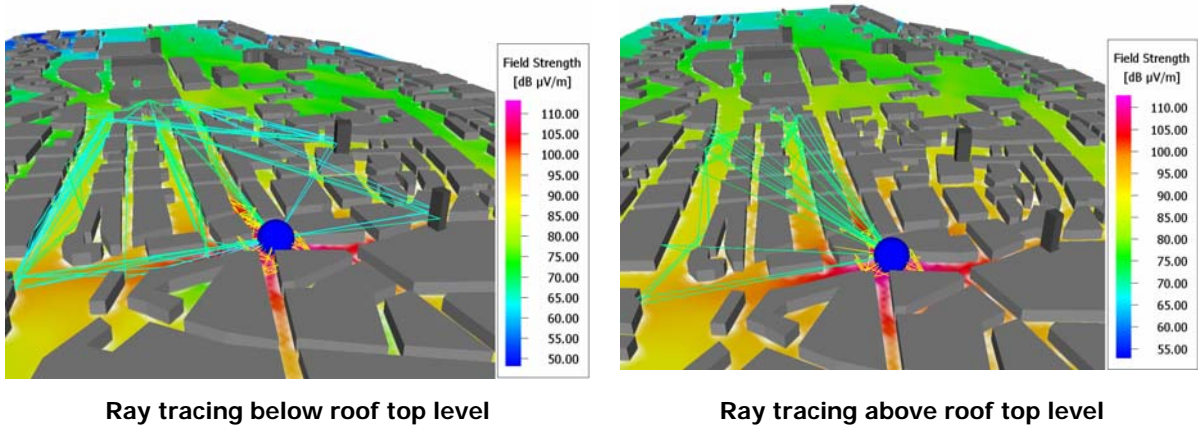


Figure 3: Ray Tracing

For base station antennas mounted below roof top level wave guiding effects in urban street canyons appear, which could reduce the angular spread at the receiving mobile stations and therefore the MIMO channel capacity, too. In environments with a lot of scatterers considerable multi path propagation appears, which can be displayed with WinProp in time and spatial domain.

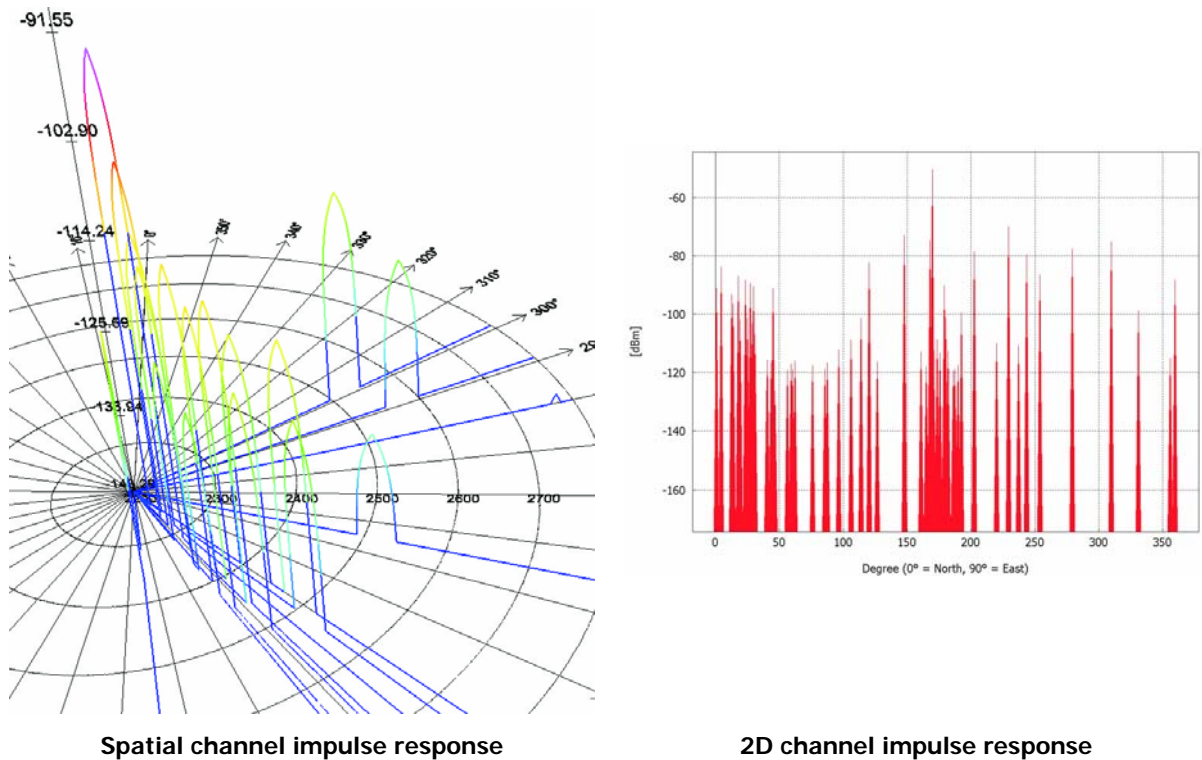


Figure 4: Channel impulse response

WinProp ray tracing has also been upgraded to compute delay and angular spreads, based on the available ray data in order to obtain all channel information needed for a complete description of MIMO channels (see Figure 5, Figure 6).

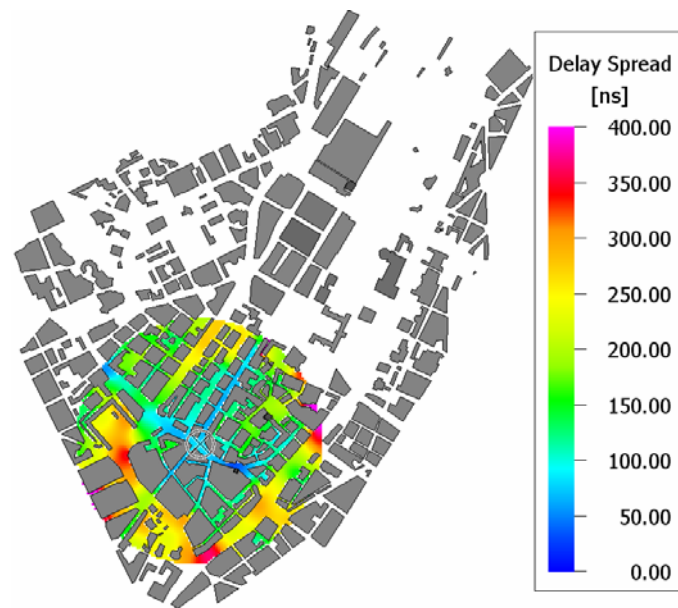


Figure 5: Delay Spread

The signal spreading in time domain is visualized by the delay spread. Especially far scatterers which provide high contributions have a significant influence on the delay spread. This parameter is important for judging about the presence of inter-symbol interference.

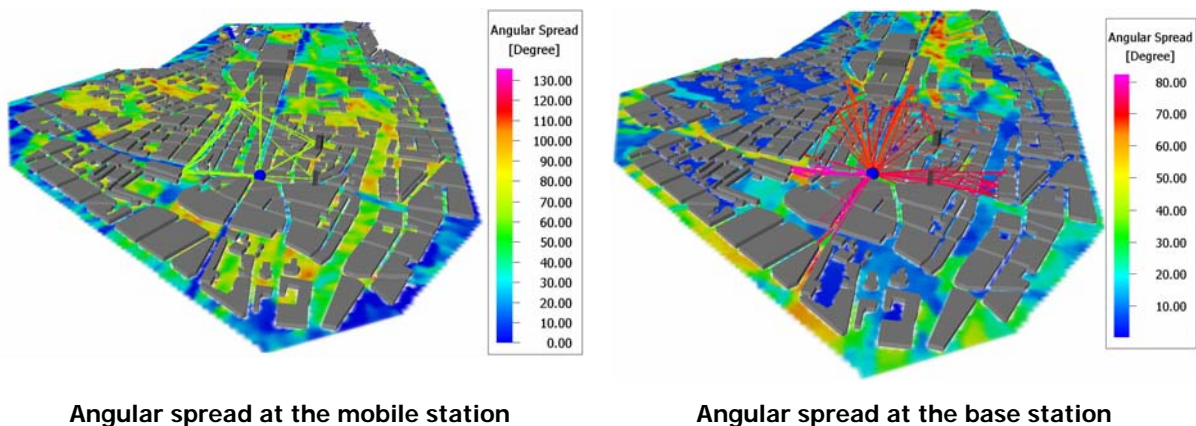


Figure 6: Angular Spread

As already mentioned, MIMO channel capacity grows linearly with antenna pairs as long as the environment has sufficiently rich scatterers. This means large channel capacities can be obtained in areas with strong multi path propagation. The multi path propagation can be expressed in terms of angular spread at the transmitter array as well as at the receiving MIMO antenna array.

WinProp is able to display those indicators for areas with strong multi path propagation in 2D and 3D maps and also in tabular ASCII files, which offers the possibility of further processing the data with other software tools. The angular spread obviously differs for each individual prediction pixel, as there are different paths for each transmitter & receiver configuration. Therefore these values are also given in form of a map for the whole simulation area.

### 3 Contribution and Superposition of Rays

There are different computation modes for the contribution and the superposition of the individual rays determined with the ray tracing algorithm. These modes can be set on the computation page of the settings menu in ProMan.

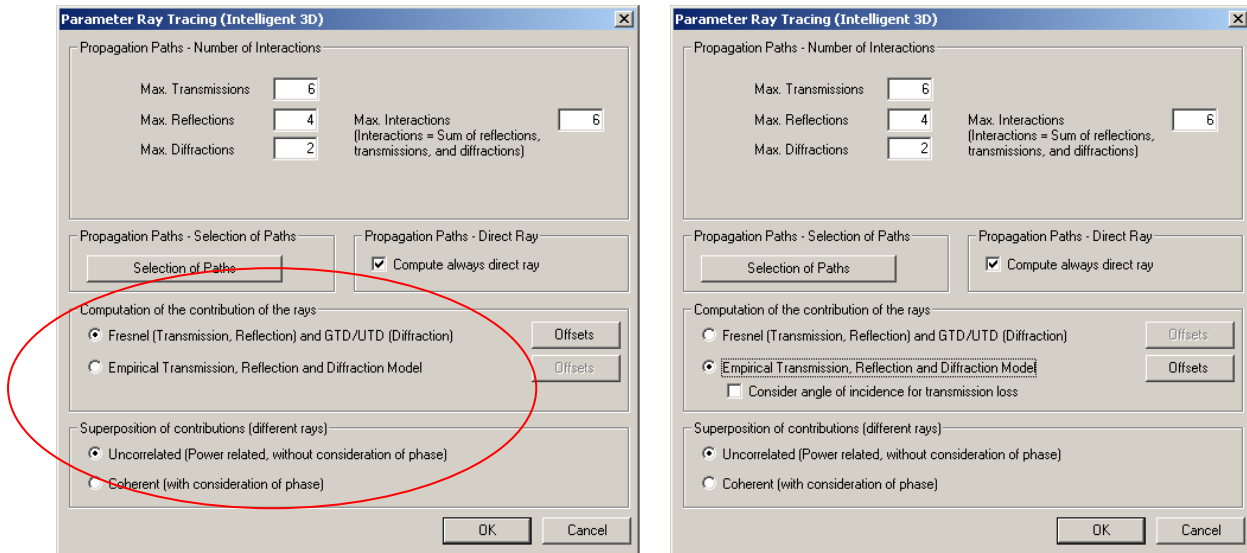


Figure 7: Ray tracing parameters

For the Fresnel and GTD/UTD mode as well as for the empirical mode (concerning the interaction modeling) combined with the uncorrelated superposition of the rays, the overall field strength of a predicted pixel is computed by summing up the contributions of the individual rays which contribute to the total field strength of this pixel, according to the following formula:

$$E_{total} = \sqrt{E_1^2 + E_2^2 + \dots + E_n^2} \quad (1)$$

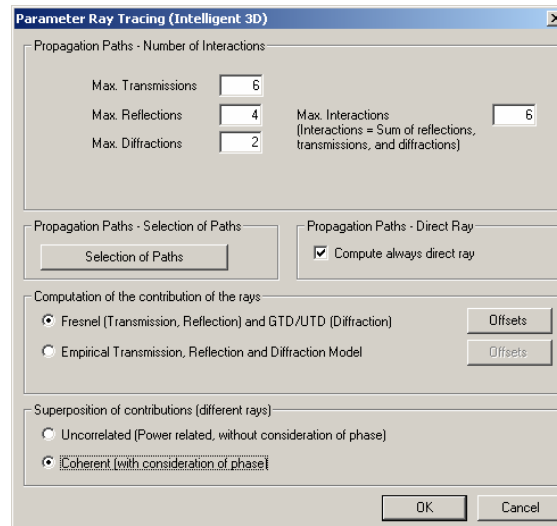


Figure 8: Ray tracing parameters

For the computation with Fresnel coefficients and GTD/UTD in combination with the coherent superposition of the rays, both the polarizations and the phases of the individual contributions are taken into account. Therefore the contributions of the individual rays are summed up separately for each polarization (real and imaginary part) first:

$$E_{x,real} = E_{1,x,real} + E_{2,x,real} + \dots + E_{n,x,real} \quad (2)$$

$$E_{y,real} = E_{1,y,real} + E_{2,y,real} + \dots + E_{n,y,real} \quad (3)$$

$$E_{z,real} = E_{1,z,real} + E_{2,z,real} + \dots + E_{n,z,real} \quad (4)$$

$$E_{x,imag} = E_{1,x,imag} + E_{2,x,imag} + \dots + E_{n,x,imag} \quad (5)$$

$$E_{y,imag} = E_{1,y,imag} + E_{2,y,imag} + \dots + E_{n,y,imag} \quad (6)$$

$$E_{z,imag} = E_{1,z,imag} + E_{2,z,imag} + \dots + E_{n,z,imag} \quad (7)$$

After that, the overall real part and the overall imaginary part are calculated by summing up the corresponding parts of the vector components:

$$E_{real} = \sqrt{E_{x,real}^2 + E_{y,real}^2 + E_{z,real}^2} \quad (8)$$

$$E_{imag} = \sqrt{E_{x,imag}^2 + E_{y,imag}^2 + E_{z,imag}^2} \quad (9)$$

Finally the total field strength of the pixel is determined according to the following formula:

$$E_{total} = \sqrt{E_{real}^2 + E_{imag}^2} \quad (10)$$

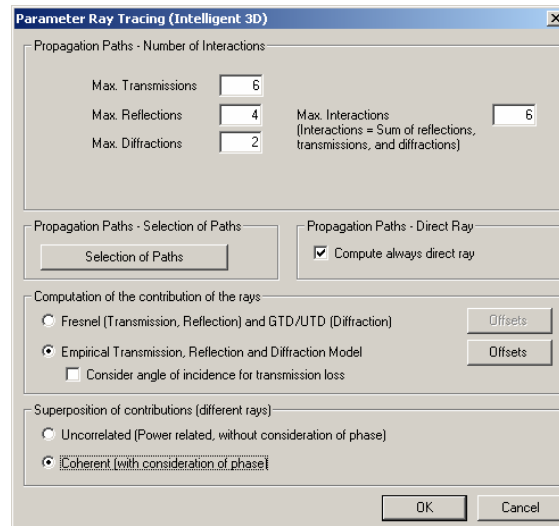


Figure 9: Ray tracing parameters

The computation with the empirical mode combined with the coherent superposition of the rays is done as follows. First the field strength components of the contributing rays are summed up for real and imaginary part separately.

$$E_{real} = E_{1,real} + E_{2,real} + \dots + E_{n,real} \quad (11)$$

$$E_{imag} = E_{1,imag} + E_{2,imag} + \dots + E_{n,imag} \quad (12)$$

After that, the overall field strength is calculated according to the following formula:

$$E_{total} = \sqrt{E_{real}^2 + E_{imag}^2} \quad (13)$$

## 4 Ray Data Files

For the purpose of post processing, WinProp's propagation tool ProMan offers the possibility to write the data corresponding to the calculated propagation paths into an ASCII (\*.str) or a binary (\*.ray) file. This optional output can be selected on the propagation page of the settings menu in ProMan (see Figure 10).

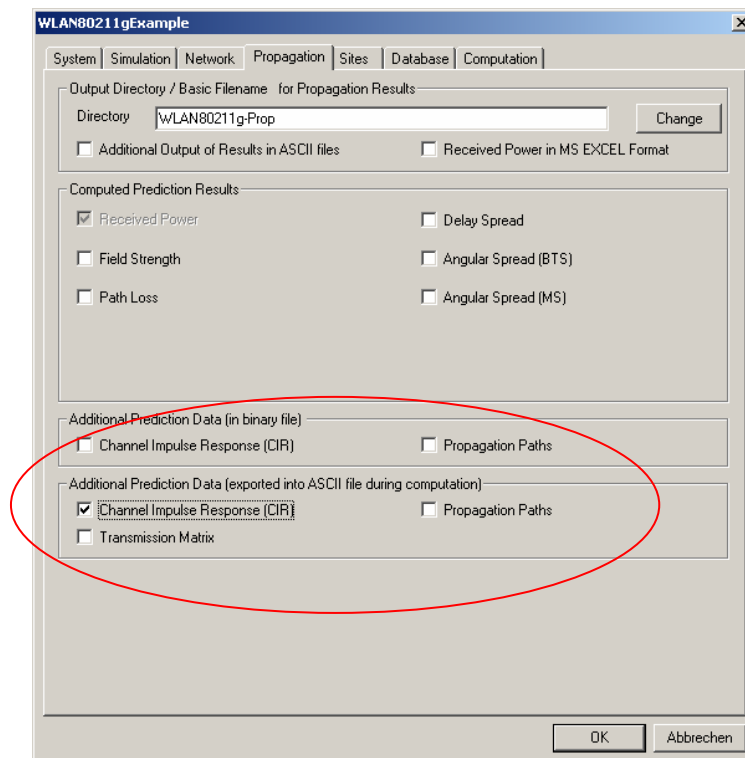


Figure 10: ProMan settings menu

There are different output alternatives within this file, depending on the selected propagation model, the computation mode, the environment under investigation and the enabled outputs on the propagation page (see Figure 10).

The output of the transmission matrix and the corresponding vector of the electrical field strength is only possible, if the standard ray tracing model (based on indoor databases) is selected in combination with the Fresnel (reflection, transmission) and GTD/UTD (diffraction) model for the calculation of the rays in indoor scenarios. Small urban scenario databases can be saved as indoor databases, in order to calculate the transmission matrix and the corresponding vector of the electrical field strength in the same way as for indoor databases. The transmission matrix is always optional, whereas the channel impulse data is always written, if the output of propagation paths is selected.

The ASCII ray file written by ProMan contains a header section with general information about the evaluated scenario, such as lower left corner, resolution of the prediction area and the specified parameters of the transmitter. After the header section the data section with the ray information for each predicted pixel starts. Coordinates of predicted pixels are indicated with the keyword POINT. Subsequent

the ray data belonging to this pixel follows indicated with the keyword PATH for each available propagation path.

```

Stgt_Site1.str - Editor
Datei Bearbeiten Format ?
LL_EDGE 3512107.00,5403384.00
HEIGHT 0.000
RESOLUTION 10.00000
COLUMNS 219
LINES 252
ANTENNA 3512882.68 5404062.63 14.00
ANTENNA_PATTERN ""
ANTENNA_HORIZONTAL 90.00
ANTENNA_VERTICAL 0.00
POWER 10.000
FREQUENCY 2000.00
CREATOR URBAN
VERSION 2
PATHS YES

*****
*** Syntax of POINT *****
*****
* POINT * x-coordinate * y-coordinate * z-coordinate
*****

*****
*** Syntax of PATH *****
*****
* PATH * Delay * FieldStrength * Type of path * Interaction points
* [ns] [dBuv/m] [0=determ. 5=empir] [X, y ,z]
*****

POINT 3512112.00 5404429.00 1.50 104
PATH 4032.740 54.77 0 2 104 0 3513019.48 5403947.49 29.50 3512183.49 5404369.25 15.00
PATH 4009.391 54.57 0 2 104 1 3513024.74 5403963.02 29.50 3512183.49 5404369.25 15.00
PATH 4099.452 54.45 0 2 104 2 3513037.27 5403958.01 29.50 3512183.49 5404369.25 15.00
PATH 4019.398 54.40 0 2 104 3 3513024.74 5403963.02 29.50 3512204.75 5404413.51 15.00
PATH 4046.083 54.20 0 2 104 4 3513019.48 5403947.49 29.50 3512204.75 5404413.51 15.00
PATH 4106.124 54.03 0 2 104 5 3513037.27 5403958.01 29.50 3512204.75 5404413.51 15.00
PATH 4469.704 53.21 0 2 104 6 3513139.98 5404171.00 30.50 3512204.75 5404413.51 15.00
PATH 4583.114 53.06 0 2 104 7 3513156.00 5404188.02 30.50 3512204.75 5404413.51 15.00
PATH 5046.763 51.23 0 2 104 8 3513019.48 5403947.49 29.50 3512482.74 5403759.48 7.50
PATH 5063.440 51.20 0 2 104 9 3513024.74 5403963.02 29.50 3512482.74 5403759.48 7.50
POINT 3512112.00 5404439.00 1.50 105
PATH 4026.069 54.25 0 2 105 0 3513024.74 5403963.02 29.50 3512204.75 5404413.51 15.00
PATH 4052.754 54.04 0 2 105 1 3513019.48 5403947.49 29.50 3512204.75 5404413.51 15.00
PATH 4112.794 53.88 0 2 105 2 3513037.27 5403958.01 29.50 3512204.75 5404413.51 15.00
PATH 4476.375 53.06 0 2 105 3 3513139.98 5404171.00 30.50 3512204.75 5404413.51 15.00
PATH 4589.786 52.91 0 2 105 4 3513156.00 5404188.02 30.50 3512204.75 5404413.51 15.00
PATH 5076.783 51.03 0 2 105 5 3513019.48 5403947.49 29.50 3512482.74 5403759.48 7.50
PATH 5093.461 51.00 0 2 105 6 3513024.74 5403963.02 29.50 3512482.74 5403759.48 7.50
POINT 3512112.00 5404449.00 1.50 106
PATH 4036.076 54.09 0 2 106 0 3513024.74 5403963.02 29.50 3512204.75 5404413.51 15.00
PATH 4062.761 53.88 0 2 106 1 3513019.48 5403947.49 29.50 3512204.75 5404413.51 15.00
PATH 4122.802 53.72 0 2 106 2 3513037.27 5403958.01 29.50 3512204.75 5404413.51 15.00
PATH 4486.381 53.56 0 2 106 3 3513139.98 5404171.00 30.50 3512158.99 5404436.50 15.00
PATH 4599.792 53.41 0 2 106 4 3513156.00 5404188.02 30.50 3512158.99 5404436.50 15.00
PATH 4486.381 52.90 0 2 106 5 3513139.98 5404171.00 30.50 3512204.75 5404413.51 15.00
PATH 4599.792 52.75 0 2 106 6 3513156.00 5404188.02 30.50 3512204.75 5404413.51 15.00
PATH 5106.803 50.97 0 2 106 7 3513019.48 5403947.49 29.50 3512482.74 5403759.48 7.50

```

Figure 11: ASCII ray file

The possible combinations of the data contained in an ASCII ray file are given in the following sub chapters for indoor (see chapter 4.1) and urban scenarios (see chapter 4.2).

### 4.1 ASCII Ray Files for Indoor Scenarios

POINT	0.0	-43.2	1.5	0
PATH	169.25	78.27	0	0

Table 1: Indoor channel impulse response

POINT	0.0	-43.2	1.5	0																
PATH	169.25	78.27	0	0	0	0	1.3e-4	-8.4e-3	8.4e-9	-5.4e-7	-8.4e-9	5.4e-7	-1.2e-4	8.2e-3	3.6e-1	-2.4e+1	2.5e+0	-1.6e+2	-1.2e+2	8.1e+3

Table 2: Indoor channel impulse response with transmission matrix

POINT	0.0	-43.2	1.5	0																
PATH	169.25	78.27	0	2	0	0	7.20	4.80	2.46	T	28	7	6.48	0.00	2.36	T	208	4		

Table 3: Indoor path data with transmission matrix

Coordinates of evaluation pixel (x, y, z)	[m]
Coordinates of interaction point (x, y, z)	[m]
Delay of path	[ns]
Field strength	[dBμV/m]
Type of path	0 = deterministic, 5 = empirical []
Number of interactions	[#]
ID of pixel	Unique ID []
ID of path	Unique ID []
Type of interaction	D = diffraction, R = reflexion, T = transmission []
ID of object where interaction occurs	Unique ID []
ID of material at the interaction point	Unique ID []
Transmission matrix Tv <sub>v</sub>	Re{Tw} Im{Tw} []
Transmission matrix Tv <sub>h</sub>	Re{Tv <sub>h</sub> } Im{Tv <sub>h</sub> } []
Transmission matrix Th <sub>v</sub>	Re{Th <sub>v</sub> } Im{Th <sub>v</sub> } []
Transmission matrix Th <sub>h</sub>	Re{Th <sub>h</sub> } Im{Th <sub>h</sub> } []
Electric field strength vector component Ex	Re{Ex} Im{Ex} [μV/m]
Electric field strength vector component Ey	Re{Ey} Im{Ey} [μV/m]
Electric field strength vector component Ez	Re{Ez} Im{Ez} [μV/m]

## 4.2 ASCII Ray Files for Urban Scenarios

POINT	0.0	-43.2	1.5	0
PATH	169.25	78.27	0	0

Table 4: Urban channel impulse response

POINT	0.0	-43.2	1.5	0								
PATH	169.25	78.27	0	2	0	0	7.20	4.80	2.46	6.48	0.00	2.36

Table 5: Urban path data

Coordinates of evaluation pixel (x, y, z)	[m]
Coordinates of interaction point (x, y, z)	[m]
Delay of path	[ns]
Field strength	[dBμV/m]
Type of path	0 = deterministic, 5 = empirical []
Number of interactions	[#]
ID of pixel	Unique ID []
ID of path	Unique ID []

## 5 Further MIMO specific Channel Parameters

### 5.1 MIMO Channel Matrix

Besides the channel characteristics described in chapter 2, MIMO systems can be evaluated in more detail by calculating the MIMO channel matrix, which describes the radio channel between each transmit and each receive antenna of the system.

There is a complex single-input-single-output (SISO) channel impulse response of length  $L+1$  between every transmit antenna  $m$  and every receive antenna  $n$  of a MIMO system.

$$h_{n,m}(t) = \sum_{l=0}^L h_{n,m,l}(t) \quad (14)$$

The linear time-variant MIMO channel is represented by the channel matrix with dimension  $N_R \times N_T$ :

$$H(t) = \begin{pmatrix} h_{1,1}(t) & \dots & h_{1,N_T}(t) \\ \dots & \dots & \dots \\ h_{N_R,1}(t) & \dots & h_{N_R,N_T}(t) \end{pmatrix} \quad (15)$$

with complex elements  $h_{n,m}(t) = \text{Re}\{h_{n,m}(t)\} + j \text{Im}\{h_{n,m}(t)\}$  (16)

The MIMO channel matrix can be determined by post-processing the ray data simulation output (see chapter 4) of the WinProp prediction tool ProMan by just calculating the phase differences between the single antenna elements of the MIMO antenna arrays at the base station and at the mobile station.

The ray data gives a description of all considered propagation paths between the position of the transmitter and each predicted receiver pixel. Field strength, delay and all interaction points (reflections, diffractions, transmissions, scatterings and turns) are listed for the single propagation paths, which contribute to the signal level at a specified location. Based on this data and the dimensions of the MIMO antenna arrays, the phase shifts between the single elements can be computed in the following way. The transmitter location given in the ray file is assumed to be the center of the transmitting MIMO antenna array. At the receiver side, the same assumption is done. Each pixel of the prediction area can be assumed to be the center point of a receiving MIMO antenna array. In order to determine the MIMO channel matrix now, only the phase shifts between the single array elements have to be computed, based on the ray data given in the ray file and on the array settings.

First of all, the angles of departure and arrival have to be computed, using the coordinates of transmitter and the first interaction point of each path and the coordinates of the last interaction point of each path and the receiver, respectively. After that, the phase shifts between the antenna elements of both arrays (see Figure 12 for example), can be easily computed.

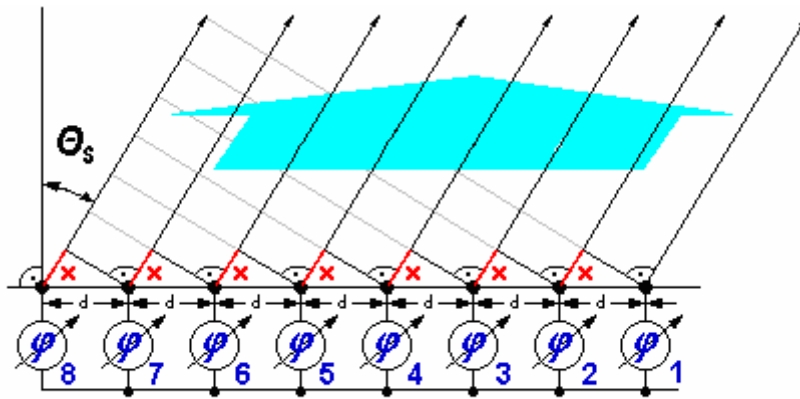


Figure 12: Uniform linear MIMO antenna array

$$\varphi = \frac{360^\circ}{\lambda} \cdot d \cdot \sin(\Theta_s) , \text{ where } \lambda \text{ is the wavelength} \tag{17}$$

The equation above holds for arbitrary adjusted uniform linear MIMO antenna arrays with antenna elements located in one horizontal plane. Based on the uniform linear array it is also possible to determine the phase shifts between the elements of a circular antenna array, by adjusting the angle of incidence in the equation above according to the location of the antenna element on the circle.

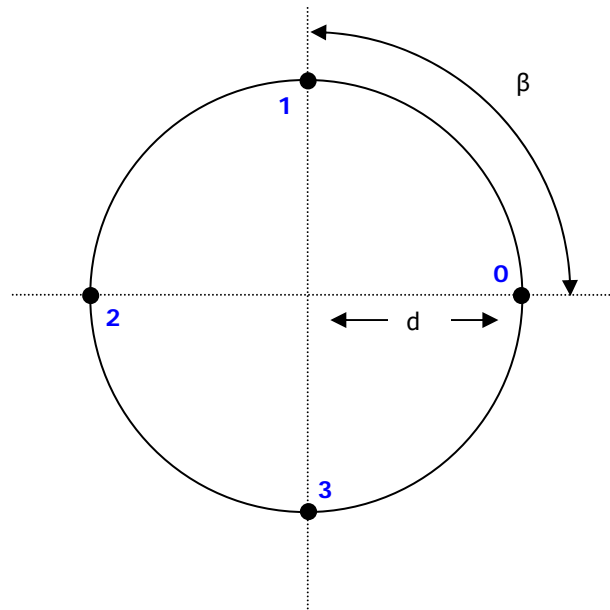


Figure 13: Circular MIMO antenna array

$$\varphi = \frac{360^\circ}{\lambda} \cdot d \cdot \sin(\Theta_s - k \cdot \beta) \tag{18}$$

Here  $\lambda$  denotes the wavelength and  $k$  the index of the antenna element ( $[0, \dots, 3]$  in this case).

## 5.2 MIMO Channel Capacity

As multiple-input multiple-output (MIMO) systems have emerged as one of the most promising approaches for high data rates, the channel capacity is another interesting parameter of a MIMO system.

The channel capacity of a non-frequency selective MIMO channel can be written as

$$C = \log_2 \left( \det \left[ I_{N_R} + \frac{P}{N_T \cdot \sigma_n^2} \cdot H_F \cdot H_F^H \right] \right) \quad [\text{bit/s/Hz}], \quad (19)$$

with the unity matrix  $I$ , the overall transmit power  $P$  and the noise power  $\sigma_n^2$ . The channel matrices  $H_F$  have to be determined by  $N_F$  point Fast Fourier Transformation. For frequency selective MIMO channels, the channel capacity can be obtained by integrating over the non-frequency selective sub channels. The mean signal-to-noise-ratio (SNR) can be expressed by  $\rho = P / \sigma_n^2$ . The resulting MIMO channel capacity for the frequency selective case can be written as follows:

$$C = \frac{1}{N_F} \sum_{l=0}^{N_F-1} \log_2 \left( \det \left[ I_{N_R} + \frac{\rho}{N_T} \cdot H_F(l) \cdot H_F(l)^H \right] \right) \quad [\text{bit/s/Hz}] \quad (20)$$

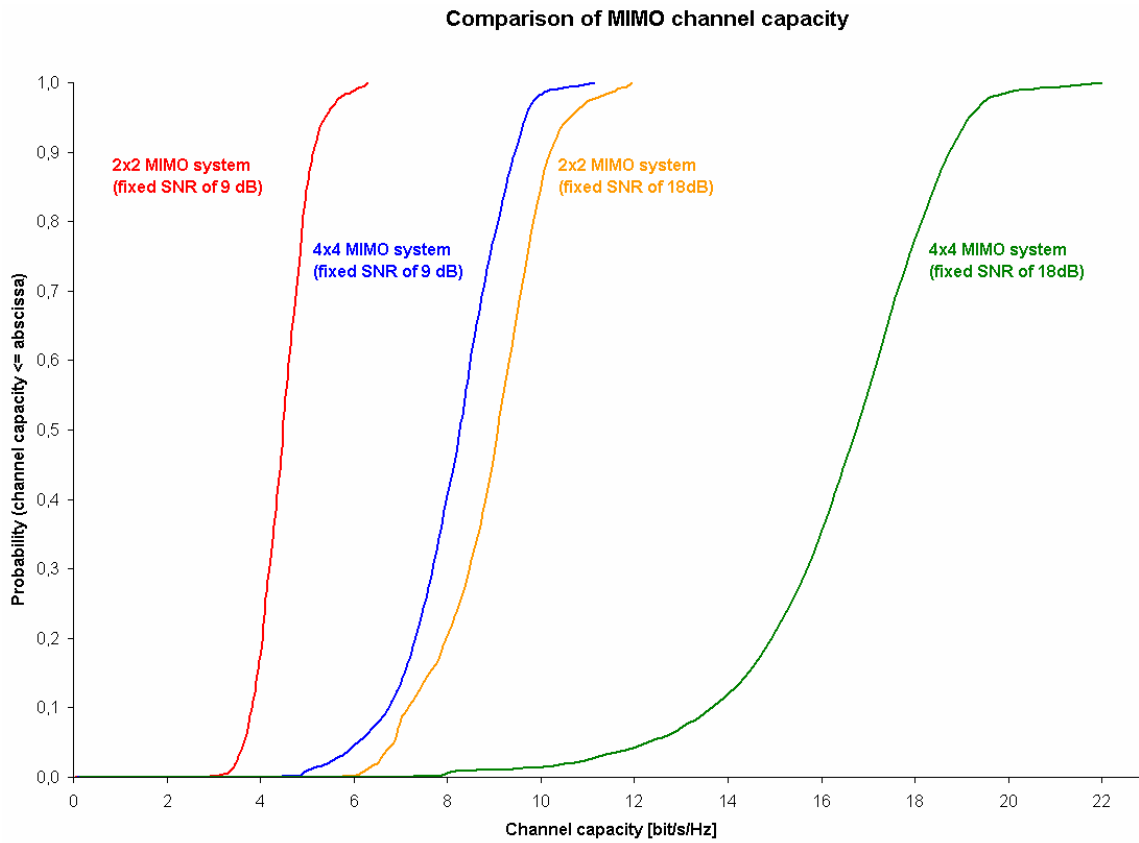
For comparison of different MIMO channels based on the same SNR, the system has to be normalized to fulfill the following condition:

$$\sum_{m=1}^{N_T} \sum_{n=1}^{N_R} \sum_{l=0}^{N_F-1} |H_{n,m}(l)|^2 = N_T \cdot N_R \cdot N_F \quad (21)$$

In order to compare different MIMO channels based on the same path loss, the system has to be normalized to fulfill the following condition:

$$\sum_{i=1}^{N_M} \sum_{m=1}^{N_T} \sum_{n=1}^{N_R} \sum_{l=0}^{N_F-1} |H_{n,m}(l,i)|^2 = N_M \cdot N_T \cdot N_R \cdot N_F \quad (22)$$

It can be shown that the MIMO channel capacity grows with antenna pairs and increasing signal-to-noise-ratio.



## 6 One Possibility to Determine Additional Channel Parameters related to MIMO Systems

AWE Communications currently develops a post-processing tool, which is able to determine additional MIMO channel parameters, based on ray data output files mentioned in previous chapters.

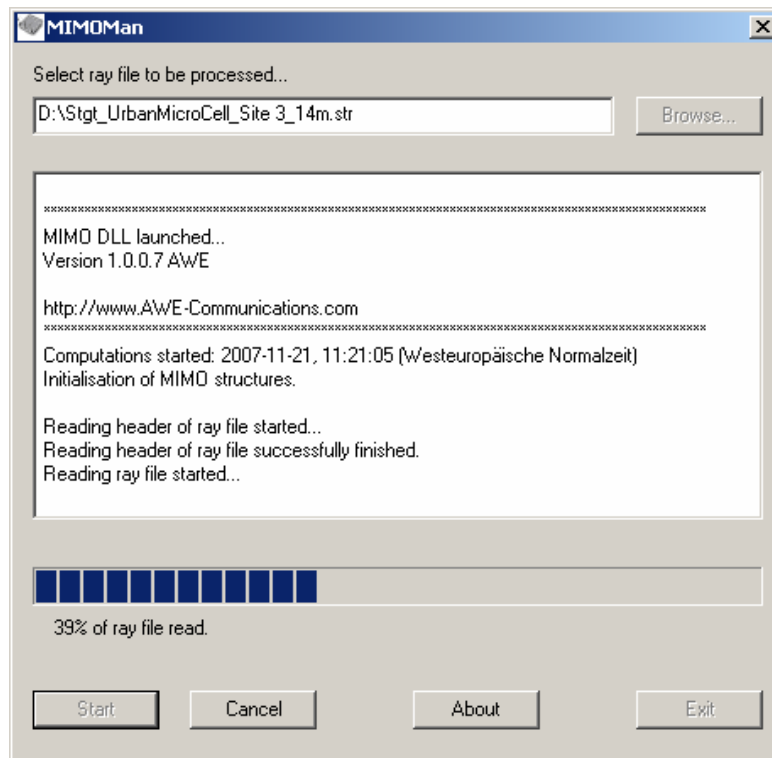


Figure 15: Post-processing tool for MIMO applications

After selecting a WinProp ray file, the post-processing starts with the specifications of the MIMO system in the configuration menu. This menu consists of five pages for the definition of the simulation area, the MIMO antenna arrays at transmitter and receiver side, and the possible output options and further settings.

### 6.1 Selections concerning the simulation area

On the first page of the configuration menu the simulation area has to be defined. The user can either investigate the whole area, which was simulated with ProMan. That means that all data contained in the loaded ray file is considered. However, this option is not recommended, because the whole prediction area is often very large and therefore a large amount of memory is allocated during post-processing.

The other options are to reduce the simulation area either in a rectangular shape or in a circular shape within the bounds of the whole prediction area stored in the ray file. If the user chooses the rectangular area, the lower left and the upper right corners of the simulation area have to be defined. The predefined values correspond to the coordinates of the whole prediction area.

For the circular area, the user has to define a center point and a radius. The whole circle has to be within the overall prediction area stored in the ray file. The predefined center coordinates of the circle correspond to the coordinates of the transmitter chosen in the ProMan propagation prediction.

With the last option on this page, special investigation points contained in a file can be loaded. This enables the user for example to specify a trajectory, which is needed to calculate velocity depending outputs like Doppler shift and Doppler spread.

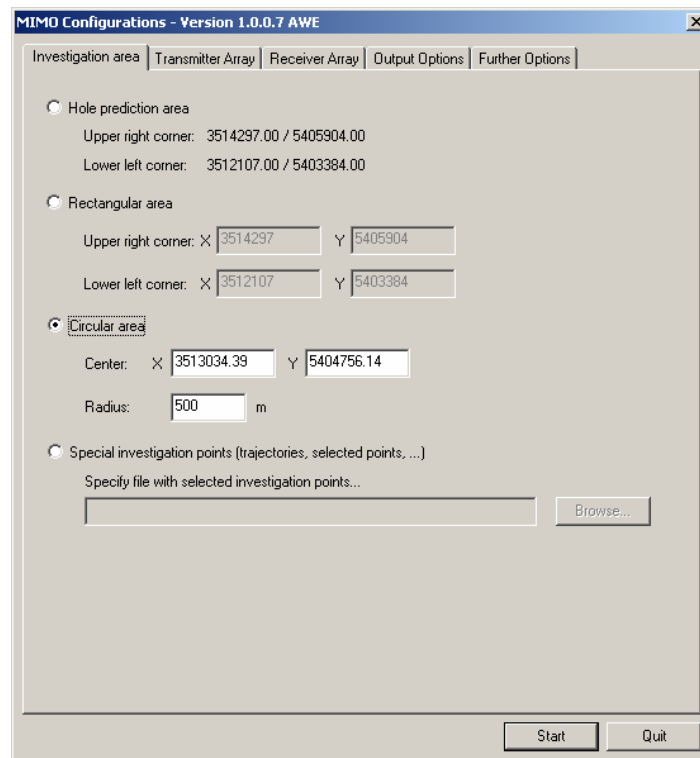


Figure 16: MIMO configuration menu – area page

## 6.2 Adjustment of the Tx MIMO Antenna Array

As already described in chapter 5, the MIMO channel matrix can be calculated based on the ray data for the center point of the antenna array and the array settings. The settings and adjustments for the transmitter antenna array can be done on the following configuration page (see Figure 17, Figure 18).

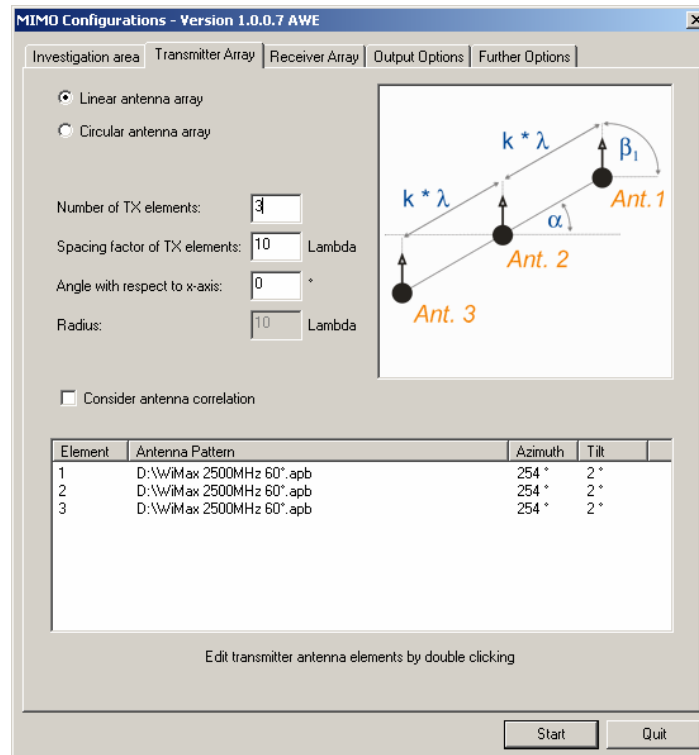


Figure 17: MIMO configuration menu – Tx array page

The user can choose a uniform linear antenna array or a circular array here (please note that all antenna elements are located in one horizontal plane). Besides the principle array type, the number of antenna elements has to be specified. For a linear antenna array, the spacing factor in wavelengths and the azimuth adjustment of the array have to be given, too. In case of a circular array, the radius of the array has to be specified in wavelengths, whereas the spacing factor is determined automatically, depending on the number of antenna elements which are equally distributed over the circle.

As an option, the correlation between the antenna elements of an array can be considered while calculating the MIMO channel matrix.

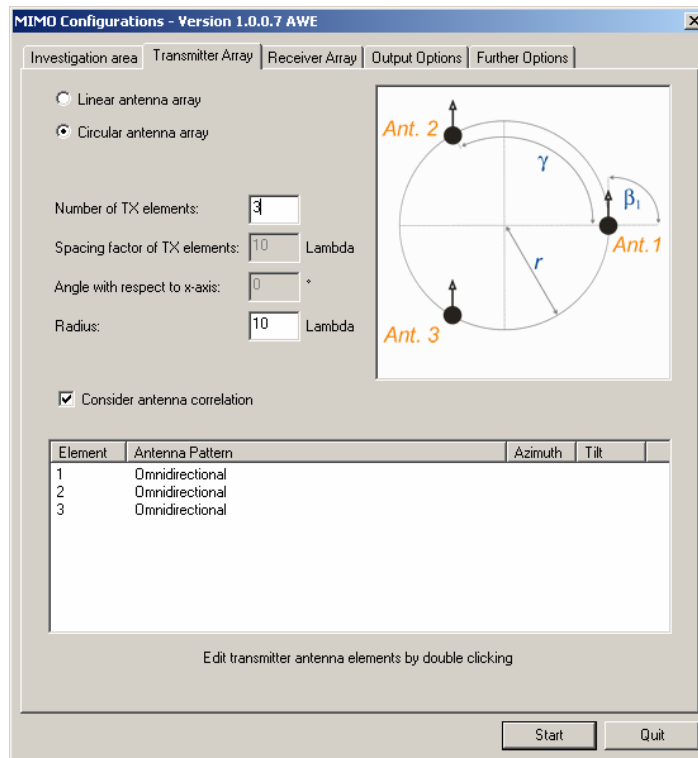


Figure 18: MIMO configuration menu – Tx array page

In the lower section of this page the single antenna elements within an array can be specified with an antenna pattern, azimuth and tilt adjustments. By default all antenna elements are considered to be omni directional isotropic radiators. By double clicking on an antenna element, the antenna adjustment dialog opens.

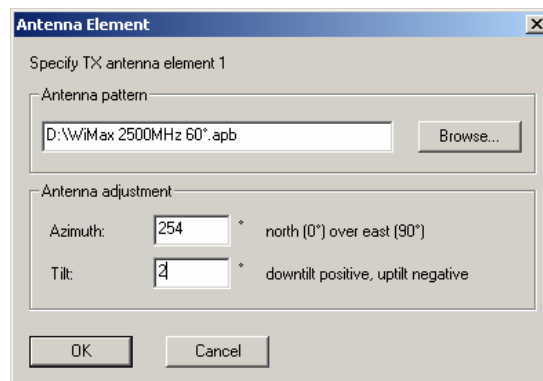


Figure 19: MIMO antenna adjustment

## 6.3 Adjustment of the Rx MIMO Antenna Array

The adjustment of the antenna array at the receiver side is done in the same way as for the transmitter antenna array. The settings and adjustments for the receiver antenna array can be done on the following configuration page (see Figure 20, Figure 21).

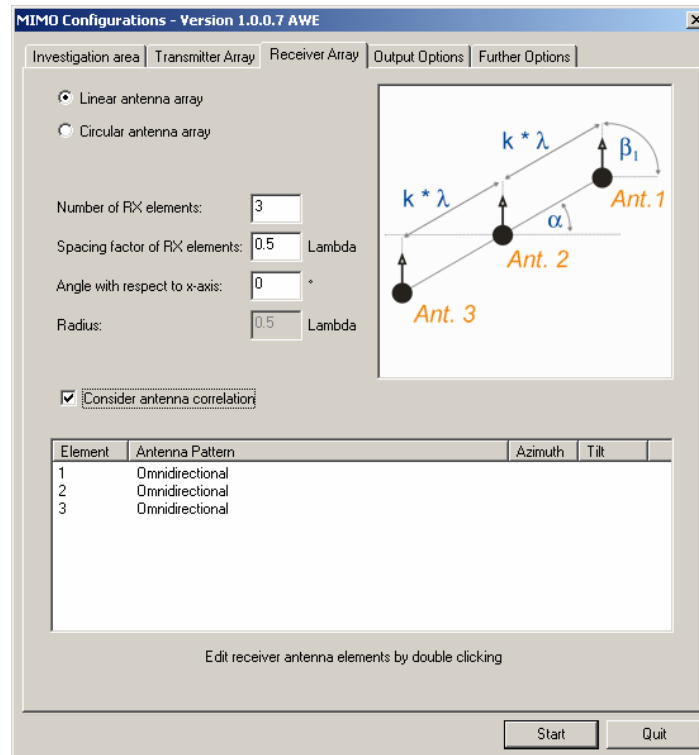


Figure 20: MIMO configuration menu – Rx array page

The user can choose a uniform linear antenna array or a circular array here (please note that all antenna elements are located in one horizontal plane). Besides the principle array type, the number of antenna elements has to be specified. For a linear antenna array, the spacing factor in wavelengths and the azimuth adjustment of the array have to be given, too. In case of a circular array, the radius of the array has to be specified in wavelengths, whereas the spacing factor is determined automatically, depending on the number of antenna elements which are equally distributed over the circle.

As an option, the correlation between the antenna elements of an array can be considered while calculating the MIMO channel matrix.

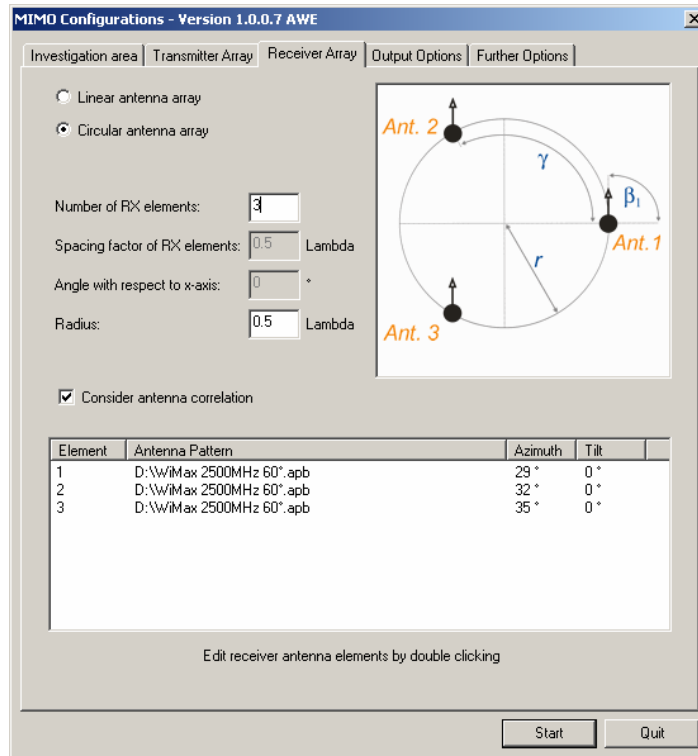


Figure 21: MIMO configuration menu – Rx array page

In the lower section of this page the single antenna elements within an array can be specified with an antenna pattern, azimuth and tilt adjustments. By default all antenna elements are considered to be omni directional isotropic radiators. By double clicking on an antenna element, the antenna adjustment dialog opens.

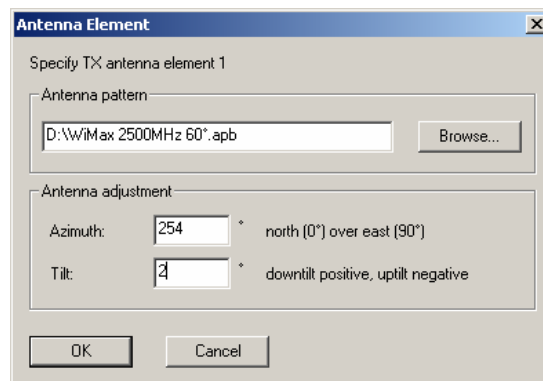


Figure 22: MIMO antenna adjustment

## 6.4 Output Options

The available outputs of the MIMO post-processing tool can be selected on the output page of the configuration menu. All results have ASCII text format and are computed for the area selected on the area page (see chapter 6.1). Due to the open ASCII format, the user is able to draw graphs with other software tools and do further evaluations.

At the beginning of the output page the user has to define a directory to store the output files. MIMO channel matrices are computed for every path of a pixel. If antenna correlation was chosen to be considered additionally (see chapter 6.2 and chapter 6.3), the matrices contain this influence, too.

The antenna correlation coefficients can be written optionally to an ASCII file either for the antenna spacing defined on the Tx and Rx array page, or for a specified range of antenna distances. For the second case a matrix or a tabular output format can be chosen. The matrix format of the antenna correlation coefficients has the following design:

$$R = \begin{pmatrix} \rho_{11} & \dots & \rho_{1N_T} \\ \dots & \dots & \dots \\ \rho_{N_R1} & \dots & \rho_{N_RN_T} \end{pmatrix} \quad (23)$$

In the tabular format, the correlation coefficients are listed with increasing distances between the elements one after the other.

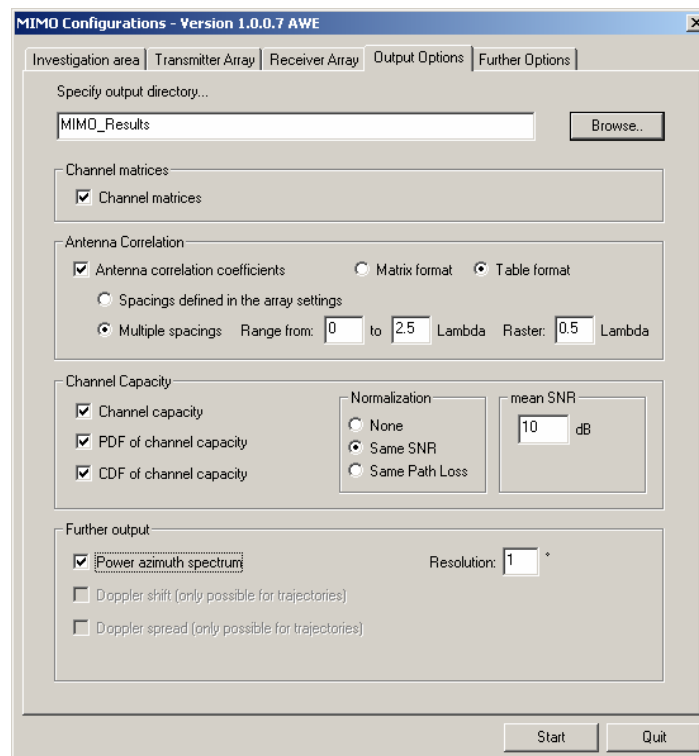


Figure 23: MIMO configuration menu – output page

The section about the channel capacity offers a general output with the capacity value of the MIMO channel at each pixel of the investigation area. Besides this, the probability density function and the cumulated probability density function of the channel capacity (whole evaluation area) can be written to an ASCII file. These values can be easily plotted with another software tool (see Figure 24).

The normalization mode for the MIMO channel capacity has to be chosen, depending on the way the user intends to compare the calculated capacities. For a comparability based on the same SNR, one has to choose "Same SNR", for a comparability based on the same path loss the last option has to be selected (see also chapter 5.2). The mean SNR to be considered during the capacity calculations has to be specified, too. As a further output the power azimuth spectrum at the transmitter antenna array as well as at the receiver array can be determined with a specified angle resolution in degrees.

Doppler shift and Doppler spread results can be only calculated for a given trajectory (see chapter 6.1) with velocity information for each point of the trajectory.

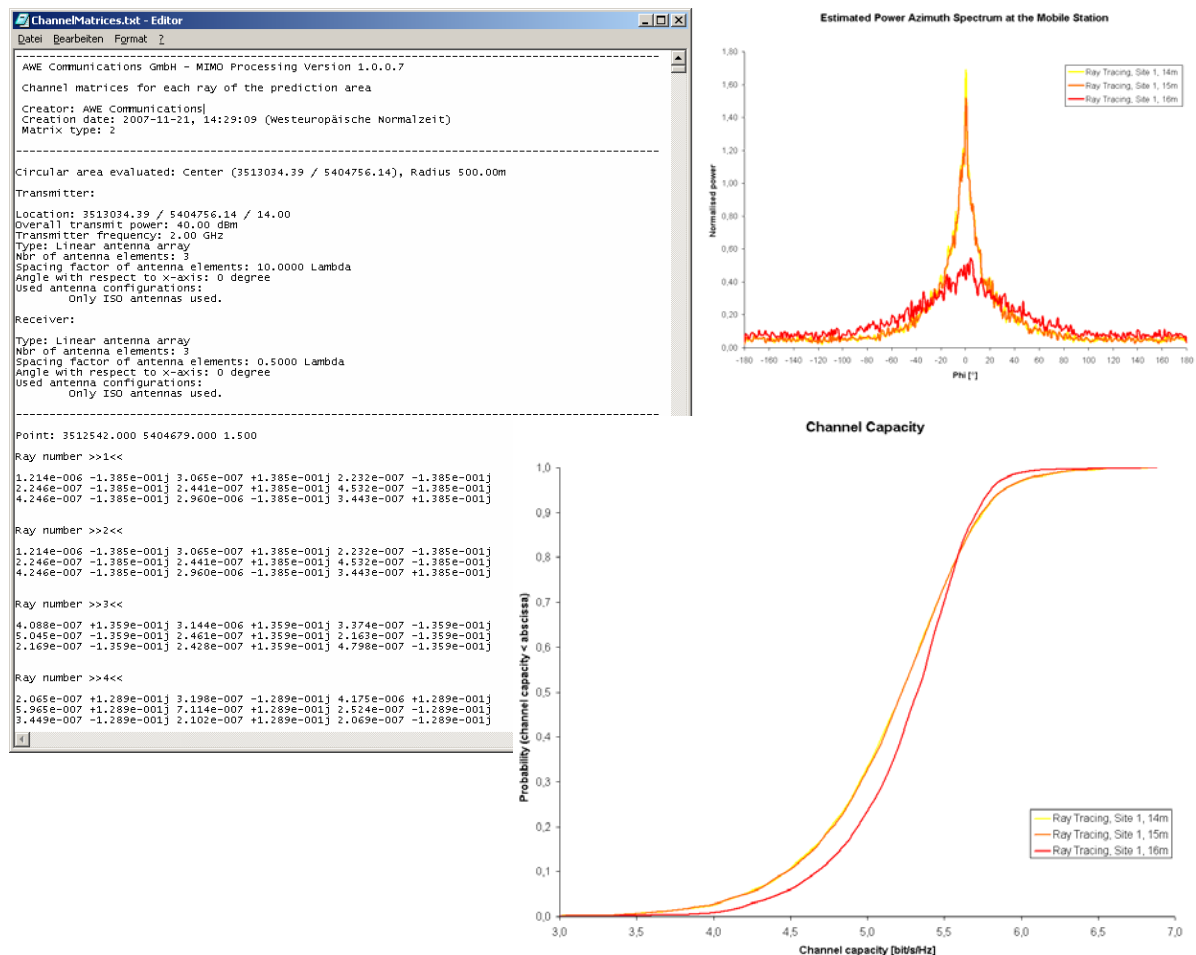


Figure 24: Sample outputs

## 6.5 Further options

On the last page of the MIMO configuration menu, the possibility of storing the configuration settings to a file is given. The user is able to store and load all or only selected configurations done on the previous pages in order to use the specified settings again for further evaluations.

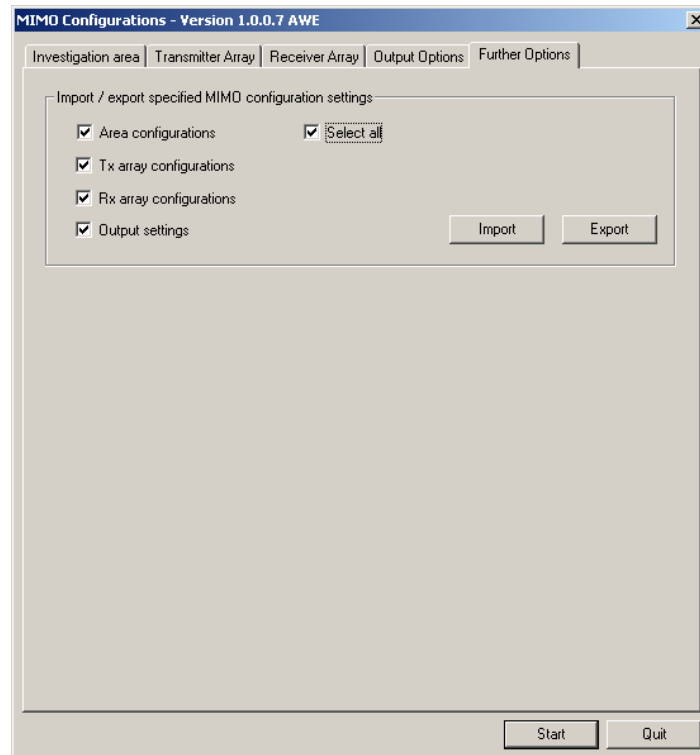


Figure 25: MIMO configuration menu – further options page

## 7 Other Applications

As already mentioned in chapter 6 the ray data output of ProMan can also be post-processed to obtain the power spectrum over the azimuth and elevation angles. This information can be used to determine direction estimation for adaptive antenna techniques, radar applications, etc.

## 8 Further Information

For further information you are invited to visit AWE Communications' website

<http://www.awe-communications.com>

or to send an e-mail to the responsible editor of this document

[Oliver.Staebler@AWE-Communications.com](mailto:Oliver.Staebler@AWE-Communications.com)

## 9 References

- [1] T. Rautiainen, G. Wölfle, and R. Hoppe: "Verifying Path Loss and Delay Spread Predictions of a 3D Ray Tracing Propagation Model in Urban Environments", 56th IEEE Vehicular Technology Conference (VTC) 2002 - Fall, Vancouver (British Columbia, Canada), September 2002.
- [2] R. Hoppe, J. Ramulu, H. Buddendick, O. Stäbler, and G. Wölfle: "Comparison of MIMO Channel Characteristics Computed by 3D Ray Tracing and Statistical Models", 2nd European Conference on Antennas and Propagation (EuCAP 2007), Edinburgh, UK, November 2007.
- [3] G. J. Foschini and M. J. Gans, "On Limits of Wireless Communication in a Fading Environment when Using Multiple Antennas," *Wireless Personal communications*, vol. 6, pp. 311–335, March 1998.
- [4] F. Hageböling, O. Weikert, U. Zölzer: "Deterministic Prediction of the Channel Capacity of Frequency Selective MIMO-Systems", Proc. 11th International OFDM-Workshop 2006 (InOWo'06), Hamburg, Germany, August 2006.